Development 138, 3803-3812 (2011) doi:10.1242/dev.062257

Differential adhesion and actomyosin cable collaborate to drive Echinoid-mediated cell sorting

Li-Hsun Chang[1], Peilong Chen[2], Mong-Ting Lien[1], Yu-Huei Ho[1], Chiao-Ming Lin[1], Yi-Ting Pan[1], Shu-Yi Wei[1] and Jui-Chou Hsu[1,3,*]

SUMMARY

Cell sorting involves the segregation of two cell populations into 'immiscible' adjacent tissues with smooth borders. Echinoid (Ed), a nectin ortholog, is an adherens junction protein in *Drosophila*, and cells mutant for *ed* sort out from the surrounding wild-type cells. However, it remains unknown which factors trigger cell sorting. Here, we dissect the sequence of this process and find that cell sorting occurs when differential expression of Ed triggers the assembly of actomyosin cable. Conversely, Ed-mediated cell sorting can be rescued by recruitment of Ed, via homophilic or heterophilic interactions, to the wild-type cell side of the clonal interface, even when differential Ed expression persists. We found, unexpectedly, that when actomyosin cable was largely absent, differential adhesion was sufficient to cause limited cell segregation but with a jagged tissue border (imperfect sorting). We propose that Ed-mediated cell sorting is driven both by differential Ed adhesion that induces cell segregation with a jagged border and by actomyosin cable assembly at the interface that smoothens this border.

KEY WORDS: Echinoid, Differential adhesion, Differential expression, Cell sorting, Actomyosin, *Drosophila*

INTRODUCTION

Cell sorting is a process in which two cell populations are smoothly partitioned into distinct adjacent tissues, similar to the phase separation between immiscible fluids. The establishment of discrete cellular compartments is key to a variety of developmental processes in different organisms, including gastrulation, neural tube formation and various types of organogenesis (Lecuit and Lenne, 2007; Perez-Pomares and Foty, 2006; Tepass et al., 2002). Cell sorting was first demonstrated when, upon mixing, dissociated presumptive neural and epidermal cells of amphibian gastrulas moved and sorted into separate tissues (Townes and Holtfreter, 1955). Cell sorting also refers to the process whereby cells in different compartments are segregated and form a smooth boundary at the compartment border (Tepass et al., 2002); for example, cells of the anterior and posterior as well as dorsal and ventral compartments of the *Drosophila* wing imaginal disc cannot intermix.

Several mechanisms have been proposed to explain the behavior of cell sorting, including differential adhesion, differential contractility and interfacial actomyosin cable formation (Martin and Wieschaus, 2010). The first hypothesis proposes that tissues with quantitatively different cell-cell adhesions have different resultant tissue surface tensions and, like dissimilar liquids, are immiscible (Steinberg, 2007). In support of this position, it has been shown that the differential expression of classic cadherins regulates the positioning of cells in the mouse telencephalon (Inoue et al., 2001) and the segregation of neurons into different motoneuron pools in the chick spinal cord (Price et al., 2002). In the second hypothesis, different levels of cell contractility are suggested to lead to differences in cell tissue surface tension and, thereby, immiscible cell populations (Harris, 1976); for example, differential contractility has been implicated in the segregation of germ layers in zebrafish (Krieg et al., 2008). The third proposal suggests that tension generated by interfacial actomyosin cables acts as a mechanical fence to prevent cell mixing, such as along the anteroposterior and dorsoventral boundaries in *Drosophila* (Landsberg et al., 2009; Major and Irvine, 2005; Major and Irvine, 2006; Monier et al., 2010).

Cadherin is the major cell adhesion molecule of adherens junctions (AJs), which mediate cell-cell adhesion/recognition. The intracellular domain of cadherin, via association with β-catenin, binds α-catenin, which in turn links to actomyosin networks. *shotgun* (*shg*) encodes *Drosophila* E-cadherin (DE-cad). Echinoid (Ed), a nectin homolog, also localizes to AJs and, via association with Canoe (Afadin), links to actomyosin (Wei et al., 2005). A common feature of these two homophilic cell adhesion molecules (CAMs) is that both *ed* and *shg* mutant clones exhibit rounded, smooth contours and sort out from surrounding wild-type cells (Laplante and Nilson, 2006; Le Borgne et al., 2002; Wei et al., 2005). This is in contrast to clones of wild-type cells, which show jagged borders. Ed-mediated cell sorting is implicated in driving various epithelial morphogenetic processes, including epithelial tube formation and dorsal closure (Laplante and Nilson, 2006; Lin et al., 2007). Ed-mediated cell sorting exhibits four characteristics (Wei et al., 2005). First, *ed* is differentially expressed in *ed* mutants and surrounding wild-type cells. Second, *ed* mutant cells accumulate a higher density of DE-cad/Armadillo (Arm; a β-catenin homolog) and develop an apical constriction (Fig. 1B). Third, *ed* mutant cells fail to form AJs with wild-type cells (Fig. 1B, arrowheads). Finally, surrounding wild-type cells confine *ed* mutant cells by assembling a ring of actomyosin cable (Fig. 1B′, arrow). However, it is currently unknown which factors are required to facilitate Ed-mediated cell sorting.

[1]Institute of Molecular Medicine, Department of Life Science, National Tsing Hua University, Hsinchu, Taiwan 30034, Republic of China. [2]Department of Physics, National Central University, Jhongli, Taiwan 32001, Republic of China. [3]Department of Biological Science and Technology, National Chiao Tung University, Hsinchu, Taiwan 30034, Republic of China.

*Author for correspondence (lshsu@life.nthu.edu.tw)

Accepted 27 June 2011

In this report, we dissect the sequence of these characteristic events during Ed-mediated cell sorting by generating *ed-RNAi* clones. We show that, following the reduction of Ed levels at the interface, the wild-type interface cells gradually assemble an actomyosin cable and form a smooth boundary. Although there was differential Ed expression, the recruitment of Ed (via homophilic and heterophilic binding) to the wild-type cell side of the clonal interface was sufficient to prevent actomyosin cable formation and thereby rescue cell sorting. Significantly, when actomyosin cable was largely absent, differential adhesion mediated by differential expression of the extracellular domain of Ed was sufficient to cause cell segregation but with jagged borders. Thus, both differential adhesion and actomyosin cable are required and collaborate to drive Ed-mediated cell sorting.

MATERIALS AND METHODS

Drosophila genetics

The following stocks were used: *C765-Gal4*, *C381-Gal4*, *en-Gal4*, *ap-Gal4*, *tubulin-Gal80^{ts}* (Bloomington Stock Center), *ed^{1X5}*, *UAS-ed* (Bai et al., 2001), *UAS-Ed$^{\Delta intra}$-Flag* (this study), *UAS-ed^{extra}-RNAi* (VDRC), *UAS-ed^{intra}-RNAi* (this study), *UAS-Ed^{TM}-cad^{intra}* (this study), *UAS-Fred-Flag* (this study), *UAS-Nrg-Ed-Flag* (this study), *tubulin-DE-cad* (Pacquelet et al., 2003), and *P[act5C>y+>Gal4] P[UAS-GFP.S65T]/CyO* (Ito et al., 1997).

To generate *ed^{1X5}* clones when endogenous DE-cad was largely downregulated, we generated *hsFLP;FRT^{40A} ed^{1X5}/FRT^{40A} ubi-nls-GFP; C765-Gal4/UAS-Ed^{TM}-cad^{intra}* larvae. To generate *UAS-Ed$^{\Delta intra}$-Flag* twinspot clones in the dorsal compartment where Ed was depleted, we generated *hsFLP; ap-Gal4,UAS-ed^{intra}-RNAi; FRT^{82B} UAS-Ed$^{\Delta intra}$-Flag/FRT^{82B} ubi-nls-GFP* larvae.

Molecular biology

UAS-ed^{intra}-RNAi was generated by subcloning exon 7 of *ed* as an inverted repeat, followed by ligation into the *pMF3* vector (Dietzl et al., 2007). *UAS-Ed^{TM}-cad^{intra}* was generated by ligating two overlapping PCR fragments, with the first PCR fragment containing the transmembrane domain of Ed and a second PCR fragment containing the intracellular domain of DE-cad, followed by ligation into *pUAST*. *UAS-Nrg-Ed-Flag* was generated by ligating two PCR fragments, with the first PCR fragment containing the fibronectin type III and transmembrane domain of Ed (with a 3′ FLAG tag) and a second PCR fragment containing the five Ig domains of Nrg, followed by ligation into *pUAST*. *UAS-Fred-Flag* was generated by inserting the *fred* PCR fragment together with a 3′ FLAG tag into *pUAST*. *UAS-Ed$^{\Delta intra}$-Flag* was generated by inserting a FLAG tag into the 3′-end of *UAS-Ed$^{\Delta intra}$* (Bai et al., 2001). *pMT-Ed*, *pMT-Fred-Flag* and *pMT-Ed$^{\Delta intra}$-Flag* plasmids were generated by respectively subcloning the *ed*, *Fred-Flag* and *Ed$^{\Delta intra}$-Flag* PCR fragments into the *pMT* vector (Invitrogen).

Endocytosis assay and S2 cell aggregation

For the endocytosis assay, third instar larvae (*en-Gal4; Ed^{TM}-cad^{intra}/tub-Gal80^{ts}*) were incubated at 29°C for 7 hours to induce *Ed^{TM}-cad^{intra}* expression. After induction, wing discs were dissected in M3 medium supplemented with 10% fetal calf serum. Discs were pulse labeled with rat anti-DE-cad for 30 minutes in ice-cold medium. After washing three times in cold M3 medium, the discs were transferred to M3 medium at 29°C for 30 minutes, followed by fixation in 4% paraformaldehyde.

For the S2 aggregation assay, S2 cells were transfected in 6-cm diameter dishes using TurboFect Reagent (Fermentas) with 4 μg *pMT-Ed*, *pMT-Fred-Flag* or *pMT-Ed$^{\Delta intra}$-Flag* vector. Transfected cells were induced overnight with 0.7 mM $CuSO_4$ and mixed, followed by incubation on a rotating shaker (20 rpm) for 4 hours at room temperature.

Histochemistry

Immunostaining was performed as described (Wei et al., 2005). Antibodies used were: guinea pig anti-Ed [1:200 (Wei et al., 2005)], rat anti-Ed [1:200 (Ho et al., 2010)], rat anti-DE-cad (DCAD2, 1:50; DSHB), guinea pig anti-Fred [1:200 (Fetting et al., 2009)], mouse anti-Arm (N2-7A1, 1:40; DSHB), rabbit anti-pSer19-MLC (1:10; Cell Signaling Technology), mouse anti-FLAG (1:500; Sigma), Alexa 594-phalloidin (1:200; Invitrogen) and Cy3- and Cy5-conjugated secondary IgGs (1:500; Jackson ImmunoResearch Laboratories). After staining, samples were mounted in 20% glycerol and nail polish was used to seal the sections. Images were acquired using 63× NA1.4 oil-immersion Plan-Apochroma objectives on a confocal microscope (LM510, Carl Zeiss).

Quantitative analysis

ImageJ software was used for quantification of apical area and of Ed and F-actin (pixel intensity). Cell bonds, connected at vertices along clone interfaces, were used to measure circularity and bond angles (determined manually) with ImageJ.

RESULTS

Differential Ed expression triggers actomyosin cable formation

ed^{1x5} null allele clones sorted out from the surrounding wild-type cells and exhibited both rounded and smooth contours (Fig. 1B). This differs from cells of the anterior and posterior compartments, which segregate and form a smooth boundary, but resembles phase separation between immiscible fluids that tend to minimize their contact surface (with the shortest interface) and have rounded and smooth interfaces (Fig. 1C). We therefore used circularity, $C=4\pi \times \text{area}/(\text{perimeter}^2)$, where perimeter is the length of clonal interface, to measure the relative roundness and smoothness of a clone (Fig. 1C) (Lawrence et al., 1999). For clones of the same apical area, that with the shortest interface (i.e. cells are immiscible) becomes a circle (C=1), whereas that with the longer interface (i.e. cells are more miscible) will deviate more from a circle and adopt a more jagged interface (Fig. 1C). Moreover, we also used the average of bond angle variation ($\overline{\Delta\theta}$, the average of bond angle differences between two adjacent bond angles) as an alternative measurement of the smoothness (but not roundness) of an interface. For a straight interface, the $\overline{\Delta\theta}=0$.

For *ed^{1x5}* mutant clones, C=0.94±0.03 and $\overline{\Delta\theta}$ =29.18±9.04° (*n*=20 clones), in contrast to control clones (Fig. 1A) where C=0.32±0.10 and $\overline{\Delta\theta}$ =88.80±16.21° (*n*=21 clones) (Fig. 1D,E). *ed* mutant cells also developed an apical constriction, with the apical area positively correlated with clone size (Fig. 1F). For example, the apical area was reduced to only 62±11% (*n*=16 clones) of that of normal cells when the clone size was less than 50 cells, whereas the apical area was 104±10% (*n*=8 clones) of that of normal cells when the clone size exceeded 150 cells (Fig. 1F). Moreover, the surrounding wild-type cells assembled a ring of actomyosin cable at the interface, with an F-actin intensity 242±28% (*n*=6 clones) of that of normal interfaces (Fig. 1G).

We used two different *ed-RNAi* constructs to silence *ed*: *ed^{extra}-RNAi* and *ed^{intra}-RNAi* against the extracellular domain and intracellular domain sequences of *ed*, respectively. Ed antibody staining confirmed that both constructs specifically inhibited *ed* expression (Fig. 1H,I). Flip-out clones overexpressing the *ed^{extra}-RNAi* or *ed^{intra}-RNAi* transgene (referred to as *ed-RNAi* clones) in the larval wing imaginal disc exhibited similar levels of circularity (Fig. 1D), average bond angle variation (Fig. 1E), apical constriction (Fig. 1F) and actomyosin cable formation (Fig. 1G) at the clonal boundary as *ed^{1x5}* mutant clones. Moreover, *ed-RNAi* clones also exhibited a lack of DE-cad at some of the clonal interfaces (Fig. 1H). We confirmed that, in wing discs, the actomyosin cable was assembled by the wild-type interface cells (Fig. 1I″, arrowhead) and was enriched in phosphorylated myosin light chain (p-MLC) (Fig. 1J), indicating that wild-type cells actively prevent mixing with the *ed* mutant cells (see below).

To distinguish the respective contributions of the four characteristics mentioned above in Ed-mediated cell sorting, we dissected the sequence of these events and determined which event led to the onset of smooth boundary formation and therefore effective cell sorting. We combined the flip-out clone with the temperature-sensitive *tub-Gal80^{ts}* driver to generate ectopic *ed^{extra}-RNAi* clones at permissive temperature (25°C) and then shifted them to restrictive temperature (29°C) for 10-22 hours to drive *ed^{extra}-RNAi* expression to differentially reduce the levels of Ed within the *ed^{extra}-RNAi* clones. Notably, *ed^{1x5}* mutant clones (starting from one *ed^{1x5}* mutant cell) tended to be round or oval in shape, whereas *ed-RNAi* clones generated by this protocol (using *Gal80^{ts}*), although with a smooth boundary, were not necessarily oval (Fig. 2B,C). It has been shown elsewhere that cell movement is insignificant in the wing disc (Gibson et al., 2006). Thus, the discrepancy in the clone shapes could be caused by the late induction of *ed-RNAi* expression after the formation of a jagged-bordered clone and the limited mobility of the *ed*-depleted cells restricted their ability to rearrange themselves into oval-shaped clones. We refer to cell sorting in this section (with reference to Fig. 2 only) as the process whereby *ed-RNAi* cells segregate from, and form a smooth border with, wild-type cells (by measuring $\overline{\Delta\theta}$), without considering the effect on clone shape, whereas the formation of rounded clones with a smooth border is a criterion of cell sorting in the remainder of the manuscript (by measuring C and $\overline{\Delta\theta}$ and comparing them with those of control and *ed^{1x5}* clones).

By shifting *ed^{extra}-RNAi* clones to the restrictive temperature for 10 hours, we observed that Ed was partially depleted in *ed^{extra}-RNAi* clones, thus establishing differential Ed expression (Fig. 2A). However, similar to wild-type control clones, the clonal boundary was jagged ($\overline{\Delta\theta}$=80.10±5.37°; *n*=8 clones) and DE-cad remained at the interface (Fig. 2A″, white lines) in these clones. Moreover, we failed to observe apical constriction of *ed^{extra}-RNAi* cells (Fig. 2A; apical area was 103±22% of that of normal cells; *n*=10 clones) and actomyosin cable formation (F-actin intensity was 102±13% of that of normal cells; *n*=6 clones). These data suggest that cell sorting had not occurred despite the obvious differential Ed expression.

Next, by shifting to restrictive temperature for 12 hours, we observed clearer differential Ed expression, but the depletion of *ed* in *ed^{extra}-RNAi* clones was not uniform (Fig. 2B). We found that the levels of Ed left at the interface negatively correlated with the levels of actomyosin cable observed (Fig. 2B,D), and that the levels of actomyosin cable at the interface were also negatively correlated with the average bond angle variation (Fig. 2E). Thus, following the reduction of Ed levels at the interface, the wild-type interface cells gradually assembled an actomyosin cable and formed a relatively smooth boundary. Of note, a weak apical constriction was also detected (Fig. 2B′,C′; apical area was 87±21% of that of normal cells; *n*=9 clones). However, DE-cad still remained on the interface (Fig. 2C) and the levels of DE-cad did not significantly change (see Fig. S1 in the supplementary material) even when Ed levels were reduced. Thus, the appearance of actomyosin cable and an apical constriction, but not the disappearance of DE-cad at the interface, were closely associated with the formation of a smooth interface.

Shifting to restrictive temperature for 22 hours completely depleted Ed in *ed^{extra}-RNAi* clones, and Ed-mediated cell sorting became very prominent ($\overline{\Delta\theta}$=44.95±17.30°; *n*=10 clones). Similar to *ed^{1x5}* mutant clones, we observed: (1) thick actin cable surrounding the entire interface (Fig. 2F′; F-actin intensity was 203±19% of that of normal cells; *n*=10 clones); (2) more obvious apical constriction of *ed^{extra}-RNAi* cells, especially in small rounded clones (Fig. 2G; apical area was 67±6% of that of normal cells; *n*=10 clones); and (3) a disappearance of DE-cad from some interfaces (Fig. 2G′, arrowhead). Thus, when the levels of Ed at the interface were further reduced, the *ed* clonal phenotype became more prominent and, importantly, the disappearance of DE-cad at the interface occurred late during this process (Fig. 2H).

Although apical constriction was detected in *ed*-depleted cells when a large number of wild-type cells surrounded a few *ed*-depleted cells (in a small *ed-RNAi* clone, Fig. 1H,I), apical constriction was also detected in wild-type cells when a large number of *ed-RNAi* cells surrounded a few wild-type cells (in a very large *ed-RNAi* clone, Fig. 2I). Moreover, apical constriction became less severe when *ed^{1X5}* clones expanded (Fig. 1F) (Wei et al., 2005) or when more wild-type cells were surrounded by a large number of *ed-RNAi* cells (compare the left and right groups of wild-type cells in Fig. 2I). Importantly, p-MLC was enriched at the clonal interface; however, we did not detect significant p-MLC accumulation in the apically constricted *ed-RNAi* cells even when the clones were small and exhibited strong apical constriction (Fig. 1J). Together, our data indicate that apical constriction is primarily, if not exclusively, a consequence, but not the cause, of cell sorting.

We showed that the disappearance of DE-cad at the interface was a late event and was, therefore, not crucial in Ed-mediated cell sorting. However, DE-cad accumulated in the apically constricted *ed-RNAi* cells, which, in turn, generated differential DE-cad expression across the *ed* clonal boundary (with higher levels in the *ed-RNAi* clone and lower levels in the surrounding cells). To determine whether differential DE-cad expression across the *ed* clonal boundary contributes to Ed-mediated cell sorting, we analyzed *ed^{1x5}* clonal phenotypes when DE-cad was removed from the epithelial cells to abolish the differential DE-cad expression. As Ed and the cell polarity protein Bazooka (Baz) mislocalize in *shg^{IG29}* null mutant cells, this indicates that DE-cad is required for the establishment/maintenance of apical-basal polarity (Wei et al., 2005). To devise a system with strongly reduced DE-cad (to abolish the differential DE-cad expression) but without complete disruption of the epithelium, we took advantage of an *Ed^{TM}-cad^{intra}* chimeric construct (with the transmembrane domain of Ed and the intracellular domain of DE-cad). We found that overexpression of *Ed^{TM}-cad^{intra}*, via *en-Gal4*, enhanced DE-cad endocytosis in the posterior compartment (Fig. 3A). Moreover, flip-out clones overexpressing *Ed^{TM}-cad^{intra}* downregulated endogenous DE-cad and caused cell sorting (Fig. 3B), similar to *shg^{IG29}* mutant clones (Wei et al., 2005). However, unlike *shg^{IG29}* mutant cells, which show no Arm association, *Ed^{TM}-cad^{intra}*-expressing cells accumulated high levels of Arm, which was probably caused by the presence of an Arm binding site in Ed^{TM}-cad^{intra} (Fig. 3C).

In addition to F-actin, several polarity markers, including Ed and aPKC, were localized normally on the *Ed^{TM}-cad^{intra}*-expressing cells (Fig. 3D,E), indicating that apical-basal polarity was largely maintained. We therefore used *C765-Gal4* to ubiquitously overexpress *UAS-Ed^{TM}-cad^{intra}* to downregulate DE-cad (but maintain Ed, Arm and F-actin distribution) in the wing disc cells and then generated *ed^{1X5}* clones in this background (for genotype, see Materials and methods). As shown in Fig. 3F, DE-cad was undetectable in cells of the *ed^{1X5}* clone (although low levels accumulated at the tricellular junctions of the surrounding wild-type cells); however, under this condition, *ed^{1X5}* clones still formed a smooth boundary (Fig. 3F and quantification in Fig. 1D,E) with

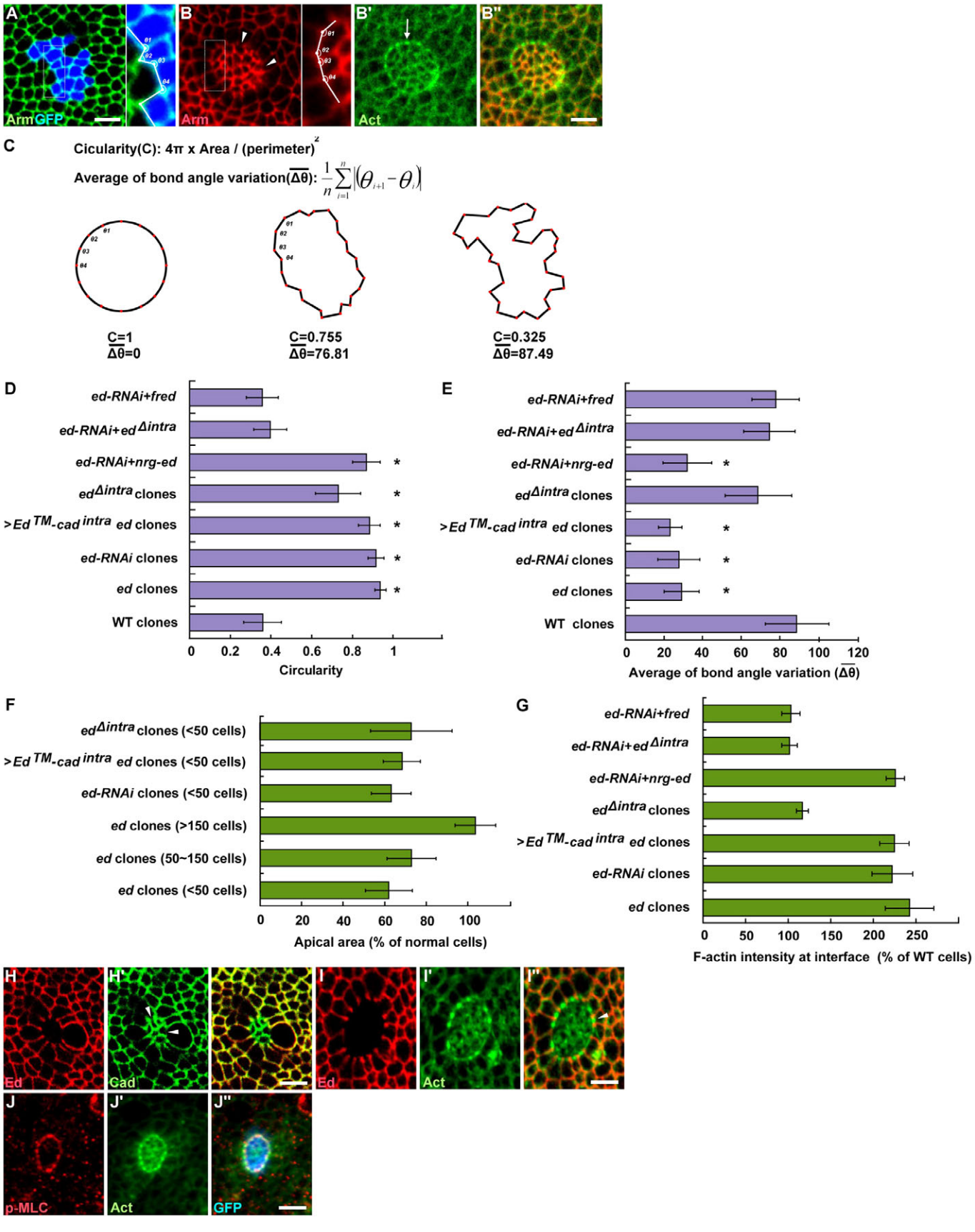

Fig. 1. See next page for legend.

Fig. 1. Phenotypes of *Drosophila ed^{1x5}* and *ed-RNAi* clones. (**A**) Wild-type clones labeled for Arm (green) and GFP (blue). The measured bond angles (clone-facing) are indicated. (**B-B″**) *ed^{1x5}* mutant clones labeled for Arm (red) and actin (green). Arrowheads indicate the lack of adherens junctions (AJs) and the arrow indicates the presence of actomyosin cable. The measured bond angles (clone-facing) are indicated. (**C**) Description of circularity C and the average of bond angle variation $\overline{\Delta\theta}$. (**D**) Quantification of circularity. From bottom to top: wild-type clones (*n*=21), *ed^{1x5}* clones (*n*=20), *ed-RNAi* clones (*n*=16), *ed^{1x5}* clones generated when DE-cad was removed (*n*=10), *Ed$^{\Delta intra}$* clones generated in the absence of Ed (*n*=20), ectopic *ed-RNAi+Nrg-Ed* clones (*n*=10), ectopic *ed-RNAi+Ed$^{\Delta intra}$* clones (*n*=15) and ectopic *ed-RNAi+fred* clones (*n*=10). Mean ± s.e.m. *, *P*<0.001 as compared with wild-type clones (paired Student's *t*-test). (**E**) Quantification of the average variation of bond angle. From bottom to top: wild-type clones (*n*=20), *ed^{1x5}* clones (*n*=20), *ed-RNAi* clones (*n*=16), *ed^{1x5}* clones generated when DE-cad was removed (*n*=5), *Ed$^{\Delta intra}$* clones generated in the absence of Ed (*n*=20), ectopic *ed-RNAi+Nrg-Ed* clones (*n*=10), ectopic *ed-RNAi+Ed$^{\Delta intra}$* clones (*n*=15) and ectopic *ed-RNAi+fred* clones (*n*=10). (**F**) Quantification of apical area. From bottom to top: *ed^{1x5}* clones with fewer than 50 cells (*n*=16), *ed^{1x5}* clones with 50-150 cells (*n*=15), *ed^{1x5}* clones with more than 150 cells (*n*=8), *ed-RNAi* clones with fewer than 50 cells (*n*=15), *ed^{1x5}* clones with fewer than 50 cells generated when DE-cad was removed (*n*=5) and *Ed$^{\Delta intra}$* clones with fewer than 50 cells generated in the absence of Ed (*n*=15). (**G**) Quantification of F-actin intensity. From bottom to top: *ed^{1x5}* clones (*n*=6), *ed-RNAi* clones (*n*=7), *ed^{1x5}* clones generated when DE-cad was removed (*n*=5), *Ed$^{\Delta intra}$* clones generated in the absence of Ed (*n*=10), ectopic *ed-RNAi+Nrg-Ed* clones (*n*=5), ectopic *ed-RNAi+Ed$^{\Delta intra}$* clones (*n*=10), ectopic *ed-RNAi+fred* clones (*n*=10). (**H-I″**) *ed^{extra}-RNAi* clones labeled for DE-cad (green in H′) and actin (green in I′); clones are marked by the absence of Ed. Arrowheads in H′ indicate the lack of AJs and arrowhead in I″ indicates actomyosin cable formation in the interface cells. (**J-J″**) *ed^{extra}-RNAi* clones labeled for p-MLC (red) and actin (green); clones are marked by the presence of GFP (blue). Scale bars: 5 μm.

actomyosin cable formation, similar to *ed^{1X5}* clones generated in the presence of DE-cad (arrowhead in Fig. 3G′ and quantification in Fig. 1G).

Together, our data indicate that when cells possess normal cell polarity with proper localization of Ed, Arm and F-actin, differential adhesion by the DE-cad extracellular domain or differential expression of DE-cad across the *ed* clonal boundary was not required for Ed-mediated smooth boundary and actomyosin cable formation. Significantly, in this case *ed^{1x5}* cells also exhibited obvious apical constriction (Fig. 3G′ and quantification in Fig. 1F), indicating that the large reduction of DE-cad-mediated adhesion or the large reduction of DE-cad (to undetectable levels) did not affect Ed-mediated apical constriction (Fig. 3G). However, we cannot exclude the possibility that a residual, very low level of DE-cad might be sufficient to contribute to Ed-mediated apical constriction.

Although we showed above that differential expression of full-length Ed triggered the assembly of actomyosin cable, which in turn led to the formation of a smooth boundary (Fig. 2D,E), differential Ed expression also causes differential Ed adhesion. It is unclear whether differential Ed expression acts solely via inducing actomyosin cable formation to drive cell sorting or, alternatively, if differential Ed adhesion also contributes to cell sorting (see below).

Rescue of Ed-mediated cell sorting

Thus far, we have shown that actomyosin cable assembles in the wild-type interface cells when differential expression of Ed occurs. To confirm this inverse correlation between Ed levels and actomyosin cable assembly, we performed rescue experiments. We found that the *ed* clonal phenotype could be fully rescued by the ubiquitous expression of *UAS-ed* using the driver *C765-Gal4*. The clones became jagged-edged and cells within the clones possessed normal levels of DE-cad (Fig. 4B). Although both Ed and DE-cad localize to AJs and might have overlapping functions (Wei et al., 2005), ubiquitous expression of DE-cad (using *tubulin-DE-cad*) failed to rescue the *ed* clonal phenotype, indicating that Ed and DE-cad are not redundant in cell recognition (Fig. 4C; data not shown).

Neuroglian (Nrg) possesses five Ig domains and heterophilically trans-interacts with Ed (Islam et al., 2003). However, unlike Ed, Nrg localizes to septate junctions of the wing disc cells (Genova and Fehon, 2003). We therefore generated *Nrg-Ed-Flag* by replacing the seven immunoglobulin (Ig) domains of Ed with the five Ig domains of Nrg, with the expectation that Nrg-Ed-FLAG might localize to the AJs and trans-interact with Ed. When ectopic clones overexpressing both *ed^{intra}-RNAi* and *Nrg-Ed-Flag* were generated, we found that Nrg-Ed-FLAG did localize to AJs in the same manner as Ed (Fig. 4D″). However, we could not detect any Ed recruited to the interface of wild-type cells (Fig. 4D), although some Nrg-Ed localized to the clonal interface (Fig. 4D′, arrowhead). This indicates that any interaction between Ed and Nrg-Ed was insufficient to recruit Ed to the interface. As expected, actomyosin cable formed and smoothed the clone boundary (Fig. 4E and quantification in Fig. 1D,E,G).

Next, we determined whether the overexpression of *Ed$^{\Delta intra}$-Flag* (comprising the transmembrane domain and the entire extracellular domain of Ed) could rescue the *ed* clonal phenotype. We generated ectopic clones overexpressing both *ed^{intra}-RNAi* and *Ed$^{\Delta intra}$-Flag* (Fig. 4F,G). We found that Ed was recruited to the clonal interface (Fig. 4F,G, arrowhead; Ed recruitment was 106±10% of that of normal cells; *n*=10 clones). Moreover, some Ed$^{\Delta intra}$-FLAG also accumulated at the clonal interface (Fig. 4F′, arrowhead), although most Ed$^{\Delta intra}$-FLAG remained localized to the interfaces between cells within the *Ed$^{\Delta intra}$-Flag*-overexpressing clones (Fig. 4F′, arrow). Similarly, Ed and Ed$^{\Delta intra}$ colocalized at the interface between S2 cells overexpressing *Ed$^{\Delta intra}$* and those overexpressing *ed* (Fig. 4H). Our results together suggest that Ed can form trans dimers with Ed$^{\Delta intra}$ (although Ed$^{\Delta intra}$ prefers to form trans homodimers). Importantly, no actomyosin cable was present at interfaces (Fig. 4G′ and quantification in Fig. 1G) and the clonal boundary was jagged (Fig. 4G and quantification in Fig. 1D,E). Thus, our data suggest that the adhesion between Ed$^{\Delta intra}$ on the *ed* mutant cells and full-length Ed on the wild-type cells was sufficient for the rescue of cell sorting. This is in sharp contrast with DE-cad, as only full-length DE-cad, but not *DE-cad$^{\Delta intra}$* (the transmembrane and the entire extracellular domain of DE-cad), can rescue the smooth contour of *shg* clones (Pacquelet et al., 2003). Thus, Ed-mediated and DE-cad-mediated cell sorting probably involve different molecular mechanisms.

Friend of Echinoid (Fred) possesses seven Ig domains and shares 69% overall sequence identity with the extracellular domain of Ed (Chandra et al., 2003). When we generated ectopic clones overexpressing both *ed^{intra}-RNAi* and *Fred-Flag*, we found that both Ed and Fred-FLAG were recruited to the clonal interface (Fig. 4I, arrowhead; Ed recruitment was 104±9% of that of normal cells; *n*=10 clones), indicating that Ed can heterophilically form trans dimers with Fred. Consistent with this, Ed and Fred colocalized to

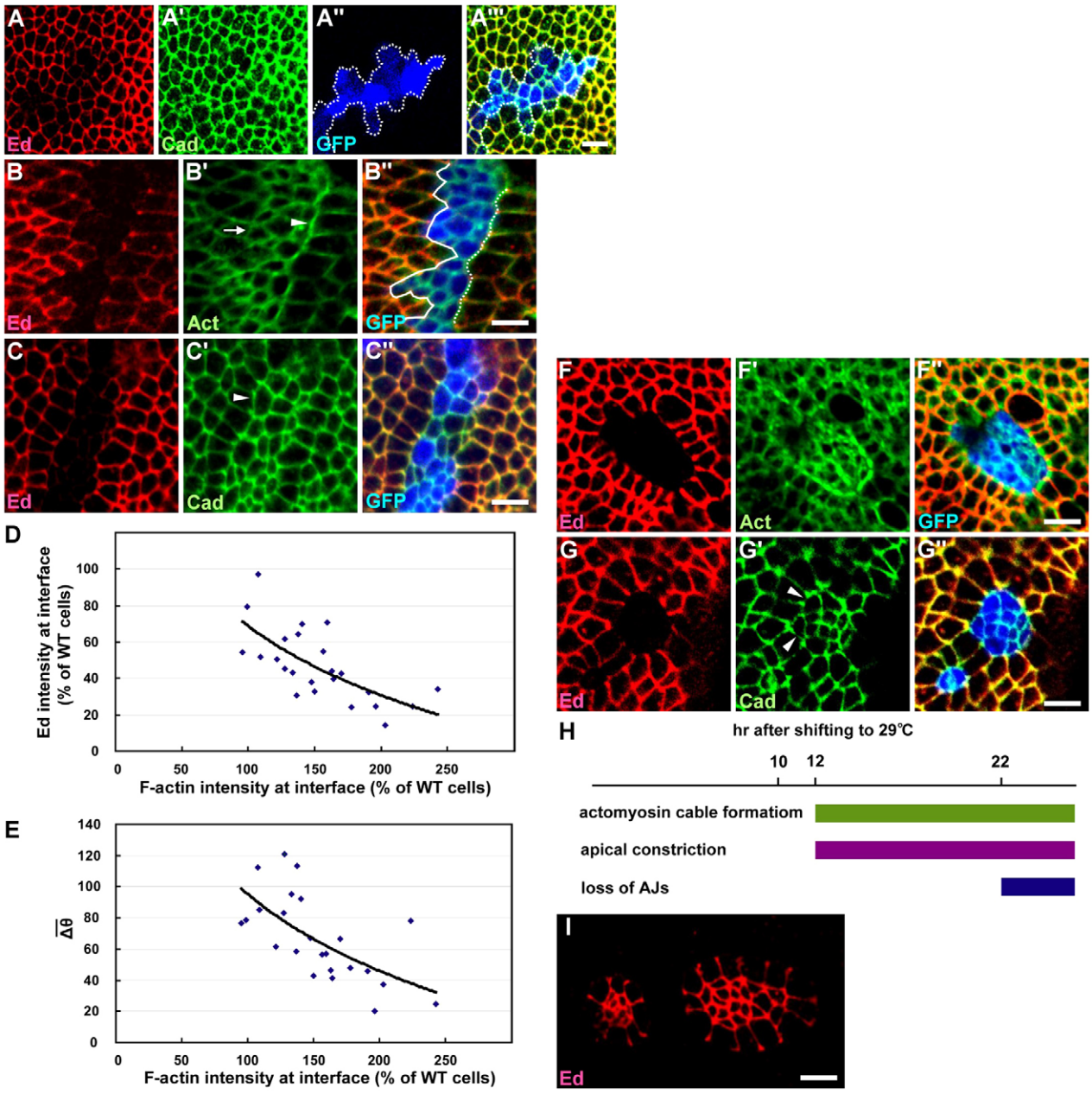

Fig. 2. Differential Ed expression is followed by actomyosin cable formation. (**A-A‴**) Ectopic *ed*^{extra}*-RNAi* clones shifted to restrictive temperature for 10 hours and labeled for Ed (red) and DE-cad (green); clones are marked by the presence of GFP (blue) and outlined by dotted lines. (**B-C″**) Ectopic *ed*^{extra}*-RNAi* clones shifted to restrictive temperature for 12 hours and labeled for Ed (red), actin (green in B′), DE-cad (green in C′); clones are marked by the presence of GFP (blue). Solid and dotted lines indicate jagged and smooth borders, respectively. Arrowhead and arrow in B′ indicate the presence and absence of actomyosin cable, respectively. Arrowhead in C′ indicates the presence of DE-cad at borders. (**D**,**E**) Correlation between Ed levels and F-actin intensity (D) and correlation between F-actin intensity and the average bond angle variation (E) at interfaces when *ed-RNAi* clones were shifted to restrictive temperature for 12 hours. Each data point represents measurements along a long border with at least nine continuous individual interfaces. (**F-G″**) Ectopic *ed*^{extra}*-RNAi* clones shifted to restrictive temperature for 22 hours and labeled for Ed (red), DE-cad (green in G′) and actin (green in F′); clones are marked by the presence of GFP (blue). Arrowheads in G′ indicate the lack of AJs. (**H**) The temporal sequence of Ed-mediated cell sorting events. (**I**) Large *ed*^{extra}*-RNAi* clones marked by the absence of Ed (red). Scale bars: 5 μm.

the interface between S2 cells overexpressing *ed* and those overexpressing *fred* (Fig. 4K, arrowheads). Similar to Ed$^{\Delta intra}$-FLAG, most Fred-FLAG localized to the interfaces between cells within the *Fred-Flag*-overexpressing clones (Fig. 4I′, arrow); thus, Fred-FLAG also prefers to form trans homodimers rather than Ed-Fred-FLAG heterodimers. Importantly, no actomyosin cable was present at the interface (Fig. 4J and quantification in Fig. 1G) and the clonal boundary was jagged (Fig. 4J and quantification in Fig. 1D,E). Thus, Ed-mediated cell sorting can be rescued by recruitment of Ed, via heterophilic interactions, to the wild-type cell side of the clonal interface, even when differential Ed expression persists. As *fred* mRNA is detected in the wing disc (Chandra et al., 2003), the failure of endogenous *fred* to rescue *ed* mutant clones indicates that the levels of endogenous Fred might

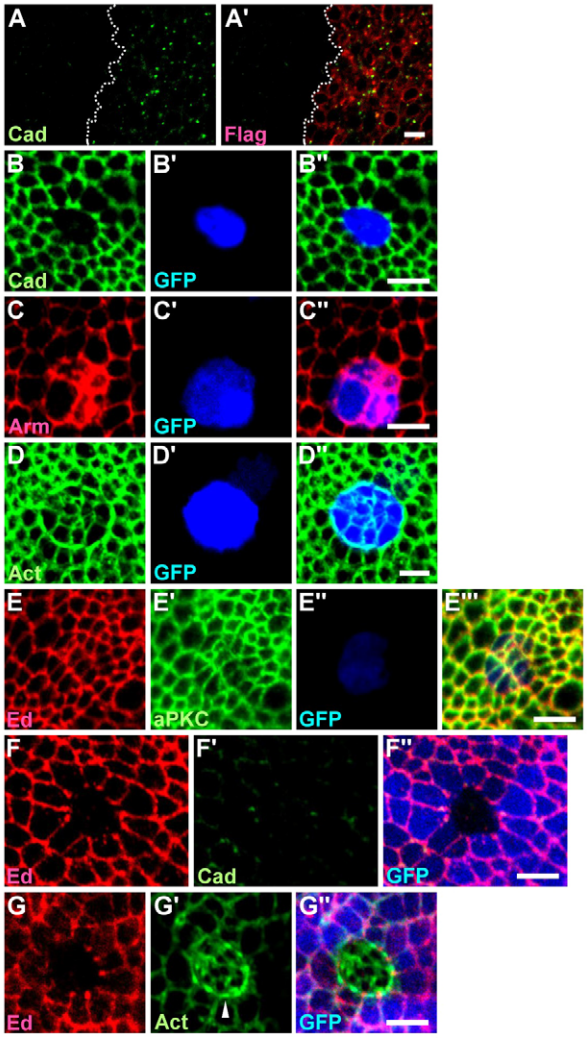

Fig. 3. Differential expression of DE-cad is not required for Ed-mediated smooth boundary formation. (**A**,**A′**) *en-Gal4*-driven *Ed*^{TM}-*cad*^{intra} in the posterior compartment (to the right of the dotted line) enhanced DE-cad endocytosis. Labeled for DE-cad (green) and FLAG (red). (**B-E‴**) Ectopic *Ed*^{TM}-*cad*^{intra} clones labeled for DE-cad (green in B), Arm (red in C), actin (green in D), Ed (red in E) and aPKC (green in E′); clones are marked by the presence of GFP (blue). (**F-G″**) *ed*^{1x5} mutant clones generated in *C765-Gal4>Ed*^{TM}-*cad*^{intra} wing disc labeled with Ed (red), DE-cad (green in F′), actin (green in G′); clones are marked by the absence of GFP (blue). Arrowhead in G′ indicates the presence of actomyosin cable. Scale bars: 5 μm.

be low and only upon ectopic overexpression can Fred heterophilically interact with sufficient amounts of Ed to recruit it to the interface. Consistent with this, using Fred antibody, we only detected Fred signals in *fred*-overexpressing but not wild-type cells (see Fig. S2 in the supplementary material). Altogether, our data indicate the importance of the presence of Ed at the clonal interface of wild-type cells to prevent actomyosin cable formation.

Differential adhesion alone causes imperfect cell sorting

We established that the differential expression of full-length Ed led to the formation of actomyosin cable and cell sorting. We were also interested in whether differential expression of Ed$^{\Delta intra}$ (the transmembrane and extracellular domains of Ed) alone would be sufficient to cause cell sorting. We generated *UAS-Ed*$^{\Delta intra}$*-Flag* twinspot clones in the dorsal compartment (where *ap-Gal4* is expressed) to drive differential Ed$^{\Delta intra}$ expression. We then examined the interface between cells without *Ed*$^{\Delta intra}$*-Flag* (with 2× *ubi-nls-GFP*) and cells with 2× *ap>Ed*$^{\Delta intra}$*-Flag* (lack of *ubi-nls-GFP*) or 1× *ap>Ed*$^{\Delta intra}$*-Flag* (with 1× *ubi-nls-GFP*). However, as full-length Ed binds Ed$^{\Delta intra}$ (Fig. 4F,G), the endogenous Ed on Ed$^{\Delta intra}$-deficient cells could still interact with Ed$^{\Delta intra}$ on the Ed$^{\Delta intra}$-containing cells (1× or 2×). This would have complicated the results, so we generated instead *UAS-Ed*$^{\Delta intra}$*-Flag* twinspot clones in the dorsal compartment where Ed was depleted by *ap-Gal4*-driven *UAS-ed*^{intra}*-RNAi* (Fig. 5A-D; for genotype see Materials and methods). Unexpectedly, we observed that the interface cells (with 2× or 1× *Ed*$^{\Delta intra}$*-Flag*) largely failed to assemble prominent actomyosin cable (Fig. 5B,C and quantification in Fig. 1G; F-actin intensity was 117±7% of that of normal cells; n=10 clones), as compared with the interface cells of *ed*^{1X5} clones (Fig. 1B and quantification in Fig. 1G; F-actin intensity was 242% of that of normal cells). Moreover, in contrast to the *ed-RNAi* clone, p-MLC was not detected at this interface (compare Fig. 5D with Fig. 1J). These data are similar to those of a recent report showing that actomyosin cable and p-MLC were not detected at the interface between *ed* (without Ed) and *ed; Ed-ΔC* (without Ed but with Ed$^{\Delta intra}$) follicle cells (Laplante and Nilson, 2011). Thus, our results indicate that this actomyosin cable, if present, must be very weak. Moreover, the presence of the intracellular domain of Ed is important for prominent actomyosin cable formation in the interface cells.

As mentioned above, it is not yet clear whether differential Ed expression acts solely by inducing actomyosin cable assembly or whether differential Ed adhesion is involved in driving cell sorting. The inability to form a prominent actomyosin cable in the Ed$^{\Delta intra}$-containing interface cells thus provided an opportunity to further evaluate the contribution of differential Ed adhesion. When actomyosin cable was largely absent, Ed$^{\Delta intra}$-deficient cells formed a coherent group, with C=0.73±0.11 (n=20 clones; lines in Fig. 5B‴′,C″). Thus, the circularity of *Ed*$^{\Delta intra}$ clones was closer to that of the *ed* mutant clones (C=0.94±0.03, Fig. 1D) but deviated more from the control clones (C=0.32±0.10), indicating that *Ed*$^{\Delta intra}$ clones sort out, to some degree, from the Ed$^{\Delta intra}$-containing cells. However, the average bond angle variation of *Ed*$^{\Delta intra}$ clones ($\overline{\Delta\theta}$=68.95±17.22°; n=20 clones) was closer to that of control clones ($\overline{\Delta\theta}$=88.80±16.21°; Fig. 1E) than to that of *ed* mutant clones ($\overline{\Delta\theta}$=29.18±9.04°), indicating the presence of jagged borders. Together, these results show that *Ed*$^{\Delta intra}$ clones exhibit effects intermediate between *ed*^{1x5} and control clones (with some cell segregation but a jagged tissue border), and we regarded this as imperfect sorting.

As we cannot completely exclude the possibility that F-actin intensity at this low level (117±7% of that of normal cells) might affect, to a small extent, the circularity of *Ed*$^{\Delta intra}$ clones, we suggest that the segregation of cells into two immiscible populations, as detected here, is mainly, if not exclusively, caused by differential adhesion of Ed$^{\Delta intra}$; however, differential adhesion of Ed$^{\Delta intra}$ is not sufficient to generate a smooth border. Of note, *Ed*$^{\Delta intra}$ clones also exhibited strong apical constriction (Fig. 5B,C and quantification in Fig. 1F). Thus, apical constriction occurred even when actomyosin cable was largely absent. Together, our results suggest that differential expression of Ed in a group of cells, via differential Ed adhesion, triggers the segregation of cells into separate populations with a jagged border and also induces the

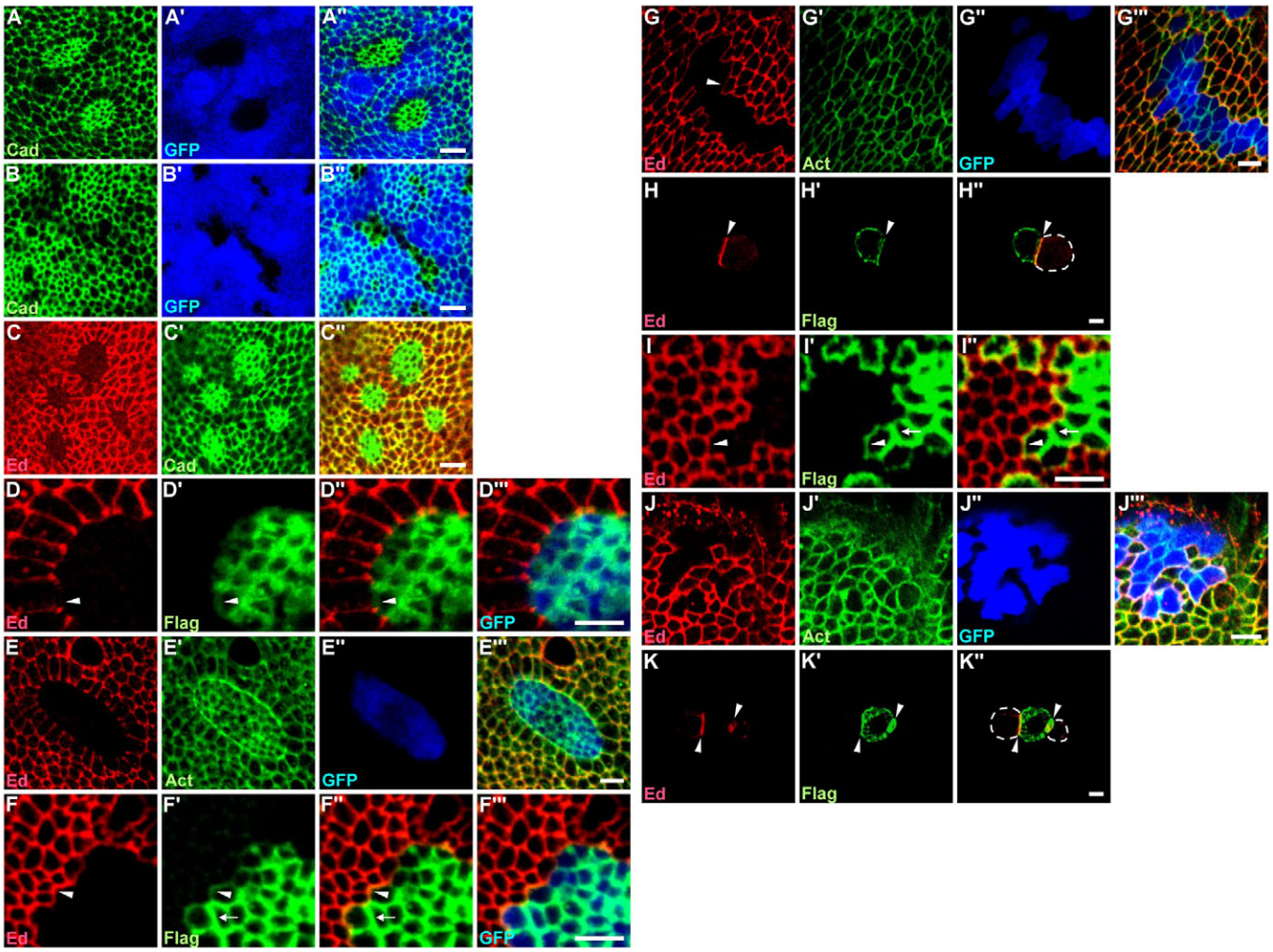

Fig. 4. Rescue of Ed-mediated cell sorting. (**A-A″**) ed^{1x5} mutant clones labeled for DE-cad (green), with clones marked by the absence of GFP (blue). (**B-C″**) ed^{1x5} mutant clones rescued by *C765-Gal4>ed* (B) and *tubulin-DE-cad* (C) labeled for DE-cad (green) and Ed (red); clones are marked by the absence of GFP (blue in B′) or Ed (C). (**D-E‴**) Ectopic clones overexpressing ed^{intra}*-RNAi* and *Nrg-Ed* labeled for Ed (red), FLAG (green in D′) and actin (green in E′); clones are marked by the presence of GFP (blue). Arrowhead in D-D″ indicates the presence of Nrg-Ed at the clone border. (**F-G‴**) Ectopic clones overexpressing ed^{intra}*-RNAi* and $Ed^{\Delta intra}$*-Flag* labeled for Ed (red), FLAG (green in F′) and actin (green in G′); clones are marked by the presence of GFP (blue). Arrowheads in F and G indicate the presence of Ed at the clone border. Arrowhead and arrow in F′ and F″ indicate the presence of $Ed^{\Delta intra}$-FLAG at the clone border and interfaces between cells within the clones, respectively. (**H-H″**) Ed and $Ed^{\Delta intra}$-FLAG colocalize to the interface (arrowhead) between S2 cells overexpressing *ed* (red, outlined by dashed lines) and S2 cells overexpressing $Ed^{\Delta intra}$*-Flag* (green). (**I-J‴**) Ectopic clones overexpressing ed^{intra}*-RNAi* and *Fred-Flag* labeled for Ed (red), FLAG (green in I′) and actin (green in J′); clones are marked by the presence of FLAG (I′) and GFP (blue in J″). Arrowheads in I and I′ indicate the colocalization of Ed (I) and Fred-FLAG (I′) at the clone border, and the arrow in I′ indicates the presence of Fred-FLAG at the interfaces between cells within the clones. (**K-K″**) Ed and Fred colocalize at the interface (arrowheads) between S2 cells overexpressing *ed* (red, outlined by dashed lines) and S2 cells overexpressing *Fred-Flag* (green). Scale bars: 5 μm.

formation of actomyosin cable at the interface, which in turn exerts tension to form a rounded clone with a smooth boundary. Thus, both differential adhesion and the induction of actomyosin cable formation are required and act cooperatively to mediate proper cell sorting.

DISCUSSION

Here, we dissect the sequence of events in Ed-mediated cell sorting and conclude that both differential adhesion and the induction of actomyosin cable formation are required and act cooperatively to mediate cell sorting. We also demonstrated that the relocalization of Ed by Ed, Fred and $Ed^{\Delta intra}$, but not Nrg-Ed, to the clonal interface of the wild-type cells is sufficient to prevent actomyosin cable formation in the wild-type cells. How differential expression of Ed induces actomyosin cable formation only at the Ed^{+} interface cells (but not the Ed^{-} cells) to generate a polarized response remains unknown. It has been suggested that interfacial tension is the result of cortical tension decreased by adhesion energy at this interface (Kafer et al., 2007; Krieg et al., 2008; Manning et al., 2010). Moreover, cortical myosin II recruitment is regulated by tension in a positive-feedback loop that could promote actomyosin cable formation (Fernandez-Gonzalez et al., 2009). Therefore, we postulated that the reduction of adhesion energy caused by the loss of Ed would increase the interfacial tension so as to induce actomyosin cable formation at that interface. However, although interfacial tension also increases in *ed* mutant cells we did not

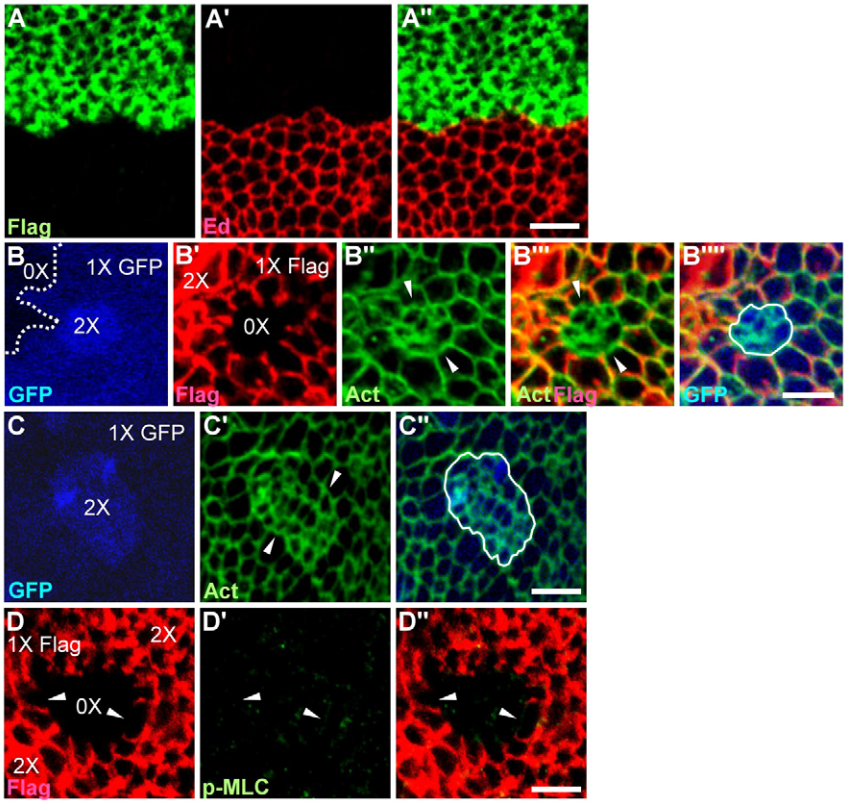

Fig. 5. Differential adhesion alone is insufficient for proper cell sorting. (**A-A″**) Ed was depleted in the dorsal compartment of *hsFLP; ap-Gal4,UAS-ed^{intra}-RNAi; FRT^{82B} UAS-Ed$^{\Delta intra}$-Flag/FRT^{82B} ubi-nls-GFP* wing disc labeled for Ed (red) and FLAG (green); dorsal compartment is marked by the presence of *Ed$^{\Delta intra}$-Flag* (green) and the absence of Ed. As expected, Ed was recruited to the interface by Ed$^{\Delta intra}$-FLAG. (**B-B‴**) Small *UAS-Ed$^{\Delta intra}$-Flag* twinspot clones generated in the absence of Ed labeled for actin (green), FLAG (red) and GFP (blue). Cells without Ed$^{\Delta intra}$-FLAG are marked by the presence of 2× ubi-nls-GFP (B) and lack of FLAG (B′). Cells with 2× Ed$^{\Delta intra}$-FLAG are marked by the lack of ubi-nls-GFP (B) and the presence of 2× FLAG (B′), whereas cells with 1× Ed$^{\Delta intra}$-FLAG are marked by the presence of 1× ubi-nls-GFP (B) and 1× FLAG (B′). Dotted (B) and solid (B‴′) lines outline the borders of the twinspot clone. Arrowheads indicate the presence of weak actomyosin cable, with F-actin intensity 113% of that of normal cells. (**C-C″**) Larger *UAS-Ed$^{\Delta intra}$-Flag* clones generated in the absence of Ed labeled for actin (green) and GFP (blue). Cells without Ed$^{\Delta intra}$-FLAG are marked by the presence of 2× ubi-nls-GFP and cells with 1× Ed$^{\Delta intra}$-FLAG are marked by the presence of 1× ubi-nls-GFP. Solid lines (C″) outline the clone borders. Arrowheads indicate the presence of weak actomyosin cable, with F-actin intensity 115% of that of normal cells. (**D-D″**) *UAS-Ed$^{\Delta intra}$-Flag* clones generated in the absence of Ed labeled for p-MLC (green) and FLAG (red). Cells without Ed$^{\Delta intra}$-FLAG are marked by the lack of FLAG and cells with 2× and 1× Ed$^{\Delta intra}$-FLAG are marked by the presence of 2× and 1× FLAG, respectively. Arrowheads indicate the absence of p-MLC at the clonal border. Scale bars: 5 μm.

detect prominent actomyosin cable formation in these cells. Thus, interfacial tension alone is insufficient to explain this polarized effect.

Laplante and Nilson (Laplante and Nilson, 2011) proposed that, during dorsal closure, asymmetric distribution of Ed is required in the dorsal-most epidermal (DME) cells for the polarized accumulation of actin regulators (such as Enabled, Diaphanous and RhoGEF2) in the actin-nucleating centers (ANCs) of DME cells, and that this in turn promotes actomyosin cable assembly at the leading edge. Ed-mediated cell sorting resembles embryonic dorsal closure, where the DME cell is equivalent to the Ed^{+} interface cell, the leading edge is equivalent to the interface of *ed* mutant clones, and the ANC is equivalent to the interfacial tricellular junction of Ed^{+} interface cells. We also found a similar polarized accumulation of actin regulators, such as Enabled, at the tricellular junction of Ed^{+} interface cells of *ed-RNAi* clones (data not shown). As cells within *ed* mutant clones cannot have a polarized distribution of Ed and actin regulators to form actomyosin cable, this provides an alternative mechanism for generating a polarized effect. Moreover, as both Nilson's group and our group demonstrated that the intracellular domain of Ed is required for actomyosin cable formation, it is possible that the asymmetric distribution of Ed might, via its intracellular domain, regulate the polarized accumulation of actin regulators at the interfacial tricellular junctions of Ed^{+} cells that in turn promotes actomyosin cable assembly.

The induction of actomyosin cable formation only at the Ed^{+} interface cells was observed not only when a large number of wild-type cells surrounded a few *ed*-depleted cells (in a small *ed-RNAi* clone, Fig. 1I,J) but also when a large number of *ed-RNAi* cells surrounded a few wild-type cells (in a very large *ed-RNAi* clone, see Fig. S3A,B in the supplementary material). The actomyosin cable at the interface supplies the tension needed to form a smooth border, tension that can be supplied either by the Ed^{+} interface cells surrounding a small *ed-RNAi* clone or by the Ed^{+} interface cells within a large *ed-RNAi* clone. However, apical constriction was present in *ed*-depleted cells surrounded by a large number of wild-type cells (in small *ed-RNAi* clones).

Similarly, apical constriction was also detected when a few wild-type cells were surrounded by a large number of *ed-RNAi* cells (in large *ed-RNAi* clones, Fig. 2I). As we did not detect significant p-MLC accumulation in the apically constricted *ed-RNAi* (Fig. 1J) or wild-type (see Fig. S3 in the supplementary material) cells, we suggest that myosin-mediated contraction is not important in the generation of apical constriction.

Ed-mediated cell sorting is similar to the process of dorsal closure. However, during dorsal closure, amnioserosa cells actively undergo pulsed contraction that leads to a reduction in their apical surfaces. This, together with the actomyosin cable acting as a ratchet, pulls the surrounding epidermal cells towards the midline (Solon et al., 2009). By contrast, the apical surface of Ed-deficient cells gradually increases when the *ed-RNAi* clones expand. Moreover, the actomyosin cable of the interface cells acts not as a ratchet but instead as a mechanical fence to smoothly separate wild-type and Ed-deficient cells. Finally, Ed-mediated cell sorting involves the polarized assembly of actomyosin cable only in the wild-type interface cells. This is in contrast to the formation of the anteroposterior boundary in the embryo, where the formation of actomyosin cable by cells on both sides of the boundary is postulated to be the primary mechanism of cell sorting (Monier et al., 2010). Here, we suggest that differential adhesion of Ed alone is sufficient to trigger the segregation of cells into separate populations with jagged borders, but it remains unknown whether differential adhesion mediated by differential expression of as yet unidentified compartment-specific CAMs plays a role in establishing the initial anteroposterior boundary, where actomyosin cable ensures that this boundary remains straight.

Acknowledgements

We thank P. Rorth, S. A. Spencer, the Developmental Studies Hybridoma Bank (DSHB), Bloomington Stock Center and Vienna *Drosophila* RNAi Center (VDRC) for providing reagents and stocks and C. Dahmann and H. Wilson for comments on the manuscript. Grants from the National Science Council, Taiwan, to J.-C.H. are acknowledged.

Competing interests statement

The authors declare no competing financial interests.

Supplementary material

Supplementary material for this article is available at http://dev.biologists.org/lookup/suppl/doi:10.1242/dev.062257/-/DC1

References

Bai, J., Chiu, W., Wang, J., Tzeng, T., Perrimon, N. and Hsu, J. (2001). The cell adhesion molecule Echinoid defines a new pathway that antagonizes the Drosophila EGF receptor signaling pathway. *Development* **128**, 591-601.

Chandra, S., Ahmed, A. and Vaessin, H. (2003). The Drosophila IgC2 domain protein Friend-of-Echinoid, a paralogue of Echinoid, limits the number of sensory organ precursors in the wing disc and interacts with the Notch signaling pathway. *Dev. Biol.* **256**, 302-316.

Dietzl, G., Chen, D., Schnorrer, F., Su, K. C., Barinova, Y., Fellner, M., Gasser, B., Kinsey, K., Oppel, S., Scheiblauer, S. et al. (2007). A genome-wide transgenic RNAi library for conditional gene inactivation in Drosophila. *Nature* **448**, 151-156.

Fernandez-Gonzalez, R., Simoes Sde, M., Roper, J. C., Eaton, S. and Zallen, J. A. (2009). Myosin II dynamics are regulated by tension in intercalating cells. *Dev. Cell* **17**, 736-743.

Fetting, J. L., Spencer, S. A. and Wolff, T. (2009). The cell adhesion molecules Echinoid and Friend of Echinoid coordinate cell adhesion and cell signaling to regulate the fidelity of ommatidial rotation in the Drosophila eye. *Development* **136**, 3323-3333.

Genova, J. L. and Fehon, R. G. (2003). Neuroglian, Gliotactin, and the Na^+/K^+ ATPase are essential for septate junction function in Drosophila. *J. Cell Biol.* **161**, 979-989.

Gibson, M. C., Patel, A. B., Nagpal, R. and Perrimon, N. (2006). The emergence of geometric order in proliferating metazoan epithelia. *Nature* **442**, 1038-1041.

Harris, A. K. (1976). Is Cell sorting caused by differences in the work of intercellular adhesion? A critique of the Steinberg hypothesis. *J. Theor. Biol.* **61**, 267-285.

Ho, Y. H., Lien, M. T., Lin, C. M., Wei, S. Y., Chang, L. H. and Hsu, J. C. (2010). Echinoid regulates Flamingo endocytosis to control ommatidial rotation in the Drosophila eye. *Development* **137**, 745-754.

Inoue, T., Tanaka, T., Takeichi, M., Chisaka, O., Nakamura, S. and Osumi, N. (2001). Role of cadherins in maintaining the compartment boundary between the cortex and striatum during development. *Development* **128**, 561-569.

Islam, R., Wei, S. Y., Chiu, W. H., Hortsch, M. and Hsu, J. C. (2003). Neuroglian activates Echinoid to antagonize the Drosophila EGF receptor signaling pathway. *Development* **130**, 2051-2059.

Ito, K., Awano, W., Suzuki, K., Hiromi, Y. and Yamamoto, D. (1997). The Drosophila mushroom body is a quadruple structure of clonal units each of which contains a virtually identical set of neurones and glial cells. *Development* **124**, 761-771.

Kafer, J., Hayashi, T., Maree, A. F., Carthew, R. W. and Graner, F. (2007). Cell adhesion and cortex contractility determine cell patterning in the Drosophila retina. *Proc. Natl. Acad. Sci. USA* **104**, 18549-18554.

Krieg, M., Arboleda-Estudillo, Y., Puech, P. H., Kafer, J., Graner, F., Muller, D. J. and Heisenberg, C. P. (2008). Tensile forces govern germ-layer organization in zebrafish. *Nat. Cell Biol.* **10**, 429-436.

Landsberg, K. P., Farhadifar, R., Ranft, J., Umetsu, D., Widmann, T. J., Bittig, T., Said, A., Julicher, F. and Dahmann, C. (2009). Increased cell bond tension governs cell sorting at the Drosophila anteroposterior compartment boundary. *Curr. Biol.* **19**, 1950-1955.

Laplante, C. and Nilson, L. A. (2006). Differential expression of the adhesion molecule Echinoid drives epithelial morphogenesis in Drosophila. *Development* **133**, 3255-3264.

Laplante, C. and Nilson, L. A. (2011). Asymmetric distribution of Echinoid defines the epidermal leading edge during Drosophila dorsal closure. *J. Cell Biol.* **192**, 335-348.

Lawrence, P. A., Casal, J. and Struhl, G. (1999). The hedgehog morphogen and gradients of cell affinity in the abdomen of Drosophila. *Development* **126**, 2441-2449.

Le Borgne, R., Bellaiche, Y. and Schweisguth, F. (2002). Drosophila E-cadherin regulates the orientation of asymmetric cell division in the sensory organ lineage. *Curr. Biol.* **12**, 95-104.

Lecuit, T. and Lenne, P. F. (2007). Cell surface mechanics and the control of cell shape, tissue patterns and morphogenesis. *Nat. Rev. Mol. Cell Biol.* **8**, 633-644.

Lin, H. P., Chen, H. M., Wei, S. Y., Chen, L. Y., Chang, L. H., Sun, Y. J., Huang, S. Y. and Hsu, J. C. (2007). Cell adhesion molecule Echinoid associates with unconventional myosin VI/Jaguar motor to regulate cell morphology during dorsal closure in Drosophila. *Dev. Biol.* **311**, 423-433.

Major, R. J. and Irvine, K. D. (2005). Influence of Notch on dorsoventral compartmentalization and actin organization in the Drosophila wing. *Development* **132**, 3823-3833.

Major, R. J. and Irvine, K. D. (2006). Localization and requirement for Myosin II at the dorsal-ventral compartment boundary of the Drosophila wing. *Dev. Dyn.* **235**, 3051-3058.

Manning, M. L., Foty, R. A., Steinberg, M. S. and Schoetz, E. M. (2010). Coaction of intercellular adhesion and cortical tension specifies tissue surface tension. *Proc. Natl. Acad. Sci. USA* **107**, 12517-12522.

Martin, A. C. and Wieschaus, E. F. (2010). Tensions divide. *Nat. Cell Biol.* **12**, 5-7.

Monier, B., Pelissier-Monier, A., Brand, A. H. and Sanson, B. (2010). An actomyosin-based barrier inhibits cell mixing at compartmental boundaries in Drosophila embryos. *Nat. Cell Biol.* **12**, 60-65.

Pacquelet, A., Lin, L. and Rorth, P. (2003). Binding site for p120/delta-catenin is not required for Drosophila E-cadherin function in vivo. *J. Cell Biol.* **160**, 313-319.

Perez-Pomares, J. M. and Foty, R. A. (2006). Tissue fusion and cell sorting in embryonic development and disease: biomedical implications. *BioEssays* **28**, 809-821.

Price, S. R., De Marco Garcia, N. V., Ranscht, B. and Jessell, T. M. (2002). Regulation of motor neuron pool sorting by differential expression of type II cadherins. *Cell* **109**, 205-216.

Solon, J., Kaya-Copur, A., Colombelli, J. and Brunner, D. (2009). Pulsed forces timed by a ratchet-like mechanism drive directed tissue movement during dorsal closure. *Cell* **137**, 1331-1342.

Steinberg, M. S. (2007). Differential adhesion in morphogenesis: a modern view. *Curr. Opin. Genet. Dev.* **17**, 281-286.

Tepass, U., Godt, D. and Winklbauer, R. (2002). Cell sorting in animal development: signalling and adhesive mechanisms in the formation of tissue boundaries. *Curr. Opin. Genet. Dev.* **12**, 572-582.

Townes, P. L. and Holtfreter, J. (1955). Directed movements and selective adhesion of embryonic amphibian cells. *J. Exp. Zool.* **128**, 53-120.

Wei, S. Y., Escudero, L. M., Yu, F., Chang, L. H., Chen, L. Y., Ho, Y. H., Lin, C. M., Chou, C. S., Chia, W., Modolell, J. et al. (2005). Echinoid is a component of adherens junctions that cooperates with DE-Cadherin to mediate cell adhesion. *Dev. Cell* **8**, 493-504.